

EVALUATION OF GLASS FIBER/EPOXY INTERFACIAL STRENGTH BY THE CRUCIFORM SPECIMEN METHOD

Jun KOYANAGI¹, Hajime KATO², Akihiro KASHIMA², Yuichi IGARASHI²,
Kenichi WATANABE³, Ichiro UENO⁴ and Shinji OGIHARA⁴

¹Institute Space and Astronautical Science, Japan Aerospace Exploration Agency

²Graduate Student, Tokyo University of Science

³Mitsubishi Rayon Co., Ltd

⁴Department of Mechanical Engineering, Tokyo University of Science
ogihara@rs.noda.tus.ac.jp

SUMMARY

The interfacial strength in a glass fiber/epoxy composite is evaluated by using the cruciform specimen method. To find the relation between the tensile and shear stresses at interfacial debonding, the angle between the fiber and the loading directions are changed. Based on the experimental data, the procedure to determine the interfacial failure criterion is discussed.

Keywords: interfacial strength, glass fiber, epoxy, cruciform specimen, debonding, interfacial failure criterion

INTRODUCTION

In fiber reinforced composite materials, the interface between the fiber and the matrix plays a key role in mechanical properties of composite materials. Therefore, a more accurate evaluation method of the interface is necessary to develop better fiber reinforced composite materials. The fragmentation test and the microbond test, etc. exist as a technique for evaluating the interfacial properties [1]. These are used to investigate the interfacial *shear* strength mainly and methods for investigating the interfacial *tensile* strength are not well established. The simplest way to evaluate the interfacial tensile strength may be to use a tensile specimen with parallel straight edges in which a through-the-width embedded fiber whose direction is perpendicular to the loading direction. However, if the fiber end appears on the free surface, stress singularity arises because the bimaterial interface is on the free surface. Even if the fiber is embedded in the matrix, the fiber end serves as the corner bimaterial interface which results in stress singularity. Therefore, it may be very difficult to evaluate the interfacial *tensile* strength accurately using this type of specimen configuration because debonding initiation is influenced by the stress singularity. Recently, an experimental method of evaluating interfacial tensile strength that uses a cruciform specimen is proposed from such a viewpoint [2-5]. In the cruciform specimen, a single fiber whose direction is perpendicular to the loading direction is embedded in the specimen central region where the specimen width is enlarged. This method can avoid the influence of interfacial stress singularity at the specimen edge on the debonding initiation. Another advantage of this method may be that it can be used to find the relation between the

tensile and *shear* stresses at interfacial debonding by changing the angle between the fiber and loading directions. This may result in experimental development of the interfacial failure criterion. In the present study, the cruciform specimen method with some different angles between the fiber and loading directions is applied on a glass fiber/epoxy composite to find the relation between the tensile and shear stresses at interfacial debonding. The procedure to determine the interfacial failure criterion is also discussed.

EXPERIMENTAL PROCEDURE

A glass fiber (17mm in the diameter) was used as the reinforcement. Epoxy resin (jER 828) was used as the matrix material with TETA (Triethylenetetramine) as a hardener. Cruciform specimens with fibers whose angles between the loading direction were 90° , 67.5° , 45° , 35° and 22.5° are used. In this work, each specimen is referred to as cruciform- α specimen, where α is the angle between the fiber and loading directions, which we refer to as *cruciform angle*. Fig.1 shows the specimen geometry. In each specimen, tension test was conducted with a small loading machine installed on the stage of an optical microscope. During loading, interfacial debonding initiation and the progress was observed. The crosshead speed was 0.05mm/min.

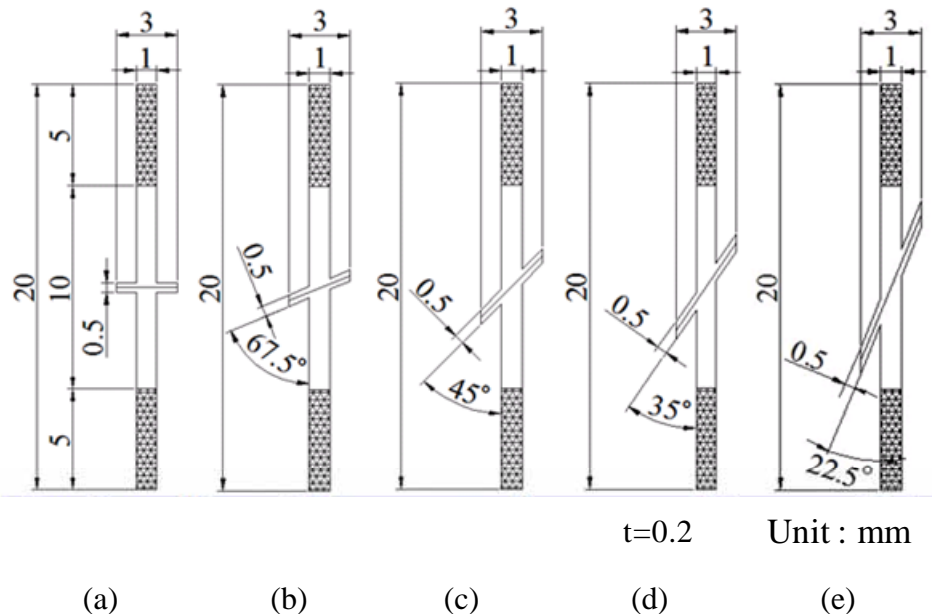


Fig.1 Schematic of cruciform specimens. (a) cruciform-90, (b) cruciform-67.5, (c) cruciform-45, (d) cruciform-35 and (e) cruciform-22.5

ANALYTICAL PROCEDURE

Finite elements analysis

The stress distribution in the specimen geometry used in the experiment was examined by finite element analysis (MSC.Marc). Effective specimen geometry was discussed for the material system used. Fig.2 shows the model of the cruciform-90 specimen. As shown in the figure, the direction of the specimen thickness was set to be the x -direction,

and the loading direction y -direction, and the direction of the specimen width z -direction, respectively. Due to symmetry about the three mutually perpendicular planes, one eighth of the model was considered for the cruciform-90 specimen. For the cruciform-67.5, cruciform-45, cruciform-35 and cruciform-22.5 specimens, half of the model was considered due to symmetry about the midplane. In each model, eight-node solid elements were used. The analysis was conducted as a linear elasticity problem. The material properties used in the analysis are shown in Table 1.

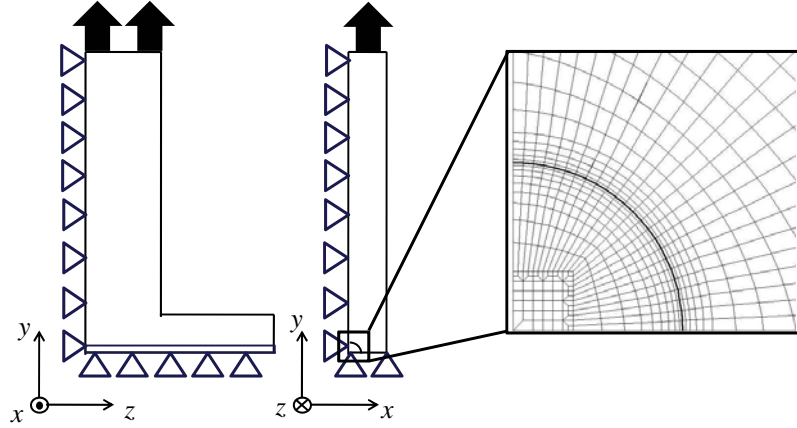


Fig.2 Schematic of a finite element analysis model (cruciform-90 specimen)

Table 1 Material properties used in the analysis

	Young's modulus [GPa]	Poisson's ratio
Glass fiber	72	0.22
Epoxy	4.28	0.42

Interfacial stresses

We considered the stress state at a point in the fiber/matrix interface. To describe the interfacial *tensile* and *shear* stresses, we define another three-dimensional Cartesian coordinate system, x' - y' - z' coordinate system, as shown in Fig.3. We take the tangential direction of the interface as x' -direction and the normal direction to the interface as y' -direction at a point in the interface as also shown in Fig.3. z' -direction coincides with z -direction. We also define the angle θ which the line from the fiber center and a point in the interface forms from the specimen thickness direction (x -direction) to specify the stress evaluation site.

The normal stress in y' -direction at an interface point, $\sigma_{y'y'}$ is the interfacial normal stress. The interfacial shear stress can be written by $\sqrt{\tau_{x'y'}^2 + \tau_{y'z'}^2}$. Because the stress we can measure is the average specimen stress, we are interested in the relation between the average specimen stress and the interfacial stresses. We defined the *normalized interfacial normal and shear stresses*, S_n and S_s , respectively, as

$$S_n = \frac{\sigma_{y'y'}}{\sigma} \quad (1)$$

$$S_n = \frac{\sqrt{\tau_{x'y'}^2 + \tau_{y'z'}^2}}{\sigma} \quad (2)$$

which are the ratio of the interfacial stresses to the average specimen stress, σ , which can be derived by the applied load and the specimen cross sectional area where the specimen width is *not* enlarged.

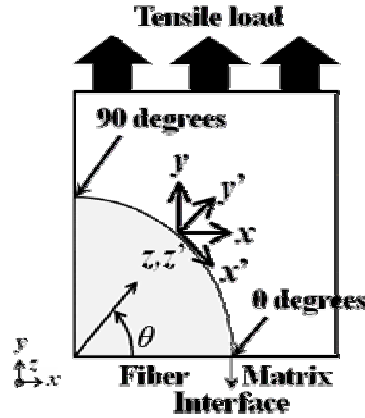
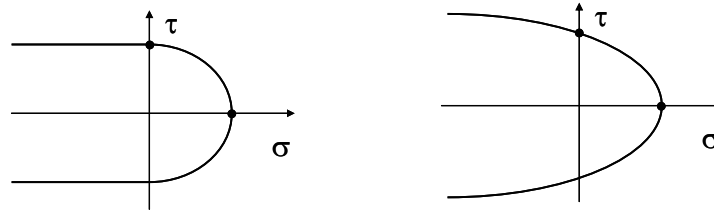


Fig.3 Stress evaluation site

INTERFACIAL FAILURE CRITERION

Although we conducted both the cruciform specimen test by varying the cruciform angles to observe the interfacial debonding initiation and FEM analysis to obtain the stress distribution to examine the relationship between the interfacial normal and shear stresses at debonding, it is very difficult to determine the point where the interfacial failure initiates because the diameter of the fiber is very small. Therefore we considered two interfacial failure criteria to discuss the point where the interfacial failure initiates, and we consider the procedure to determine the interfacial failure criterion based on the experimental results. Fig.4 shows schematics of (a) the quadratic failure criterion and (b) parabolic failure criterion which are described by



(a) Quadratic failure criterion

(b) Parabolic failure criterion

Fig.4 Schematic of interfacial failure criteria. (a) Quadratic failure criterion and (b) parabolic failure criterion.

$$\left(\frac{\langle t_n \rangle}{Y_n}\right)^2 + \left(\frac{t_s}{Y_s}\right)^2 = 1 \quad (3)$$

$$\frac{t_n}{Y_n} + \left(\frac{t_s}{Y_s} \right)^2 = 1 \quad (4)$$

where t_n is interfacial normal stress, t_s interfacial shear stress, Y_n the interfacial tensile strength, Y_s the interfacial shear strength, and $\langle \cdot \rangle$ is the McAuley bracket with its usual definition $\langle x \rangle = \frac{1}{2}(x + |x|)$.

RESULT AND DISCUSSION

Experimental results

Figure 5 shows the initiation and progress of the interfacial debonding observed in (a) cruciform-90 and (b) cruciform-67.5 specimens. Similar debonding initiation and progress behavior is also observed in cruciform-45 and cruciform-35 specimens. However, in Cruciform-22.5 specimens, no debonding initiation was observed, that is, specimen final fracture occurred before the debonding initiation. Table 2 shows the averaged specimen average stress at interfacial debonding. It can be seen that as the cruciform angle gets smaller, the debonding initiation specimen average stress gets higher. In cruciform-22.5 specimen, it can be considered that the average specimen stress at interfacial debonding is higher than 36.1 MPa.

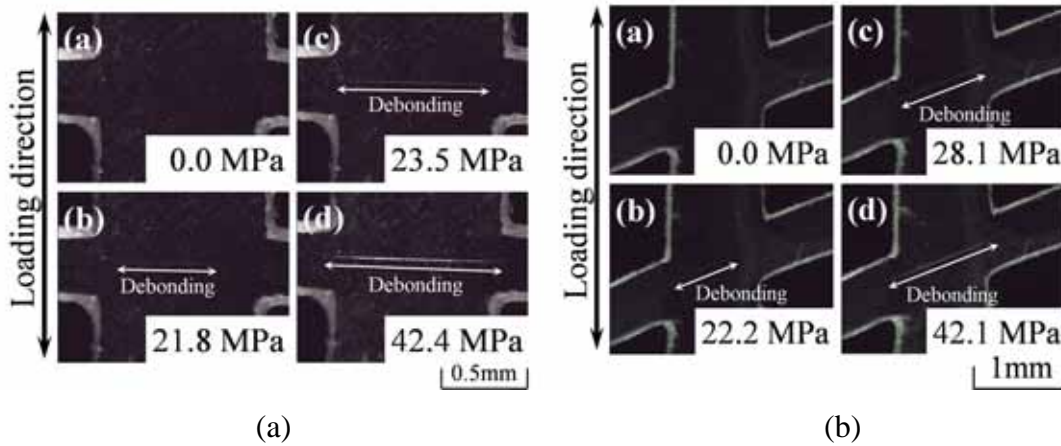


Fig.5 Debonding initiation and progress in (a) Cruciform-90 and (b) Cruciform-67.5 specimens

Table 2 Debonding stress in cruciform-90, 67.5, 45, 35 and 22.5

Specimen type	Debonding stress [MPa]
Cruciform-90	17.6
Cruciform-67.5	20.1
Cruciform-45	29.4
Cruciform-35	33.6
Cruciform-22.5	36.1 (Specimen Failure)

Analytical results

Figure 6 shows the changes in (a) the normalized normal stress and (b) the normalized shear stress along the fiber in the cruciform-90 specimen. In Fig.6 (a), the normalized normal stress is highest at $\theta=90^\circ$, but Fig.4 (b) shows that the normalized shear stress is highest at $\theta=45^\circ$. A similar result was obtained in the cruciform-67.5 specimen. Therefore it is not possible to determine the point (θ) where the interfacial debonding initiates from the stress distributions because the interfacial failure criterion under mixed-mode (combined) stress state is not developed.

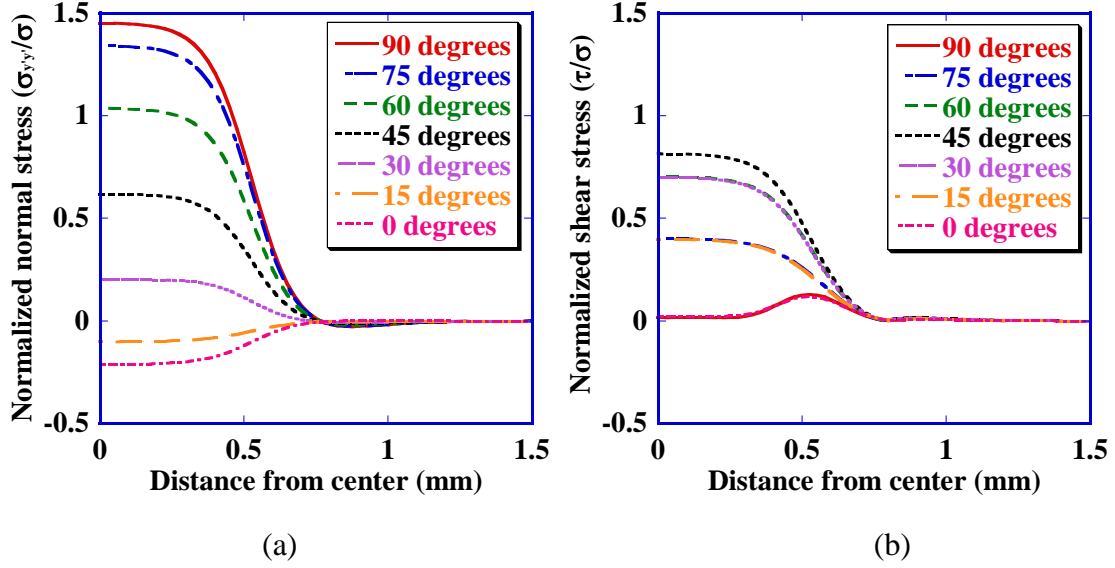


Fig.6 Change in the normalized stresses along the fiber direction. (a) Distribution of normalized tensile stress and (b) distribution of normalized shear stress.

Interfacial failure criteria

It is necessary to determine the point where the interfacial debonding initiates. In the present study, we considered two interfacial failure criteria as shown in Fig.4. First, the quadratic failure criterion is considered. Equation (3) can be rearranged to

$$Y_n = \sqrt{\langle t_n \rangle^2 + \left(\frac{t_s}{\alpha} \right)^2} \quad (5)$$

where we introduced a parameter α which can be defined by

$$\alpha = \frac{Y_s}{Y_n} \quad (6)$$

which is the ratio of the interfacial shear strength, Y_s , to the interfacial tensile strength, Y_n . Normalized interfacial normal and shear stresses can be written by

$$k_n(\theta) = t_n(\theta) / \sigma_{spe} \quad (7)$$

$$k_s(\theta) = t_s(\theta) / \sigma_{spe} \quad (8)$$

where σ_{spe} is the average specimen stress, and both the normalized interfacial stresses and the interfacial stresses are expressed explicitly as functions of the angle θ . Equations (7) and (8) are substituted into equation (6) which results in

$$Y_n = \sqrt{\{k_n(\theta)\}^2 + \left\{\frac{k_s(\theta)}{\alpha}\right\}^2} \cdot \sigma_{spe} \quad (9)$$

where the relation between the interfacial tensile stress, Y_n , and the experimentally-obtained average specimen stress at interfacial debonding, σ_{spe} . Now, we define a function $F(\alpha, \theta)$ as

$$F(\alpha, \theta) = \sqrt{\{k_n(\theta)\}^2 + \left\{\frac{k_s(\theta)}{\alpha}\right\}^2} \quad (10)$$

and we refer to as the equivalent normalized interfacial stress. In the parabolic failure criterion, $F(\alpha, \theta)$ can be written as

$$F(\alpha, \theta) = \frac{k_n(\theta) + \sqrt{\{k_n(\theta)\}^2 + 4\left\{\frac{k_s(\theta)}{\alpha}\right\}^2}}{2} \quad (11)$$

In a specific failure criterion, it can be considered that θ which gives the maximum $F(\alpha, \theta)$ with given α is the interfacial failure initiation location.

Figures 7 and 8 show F as a function of θ with some assumed value of α for the cruciform-90 and cruciform-45 specimens, respectively, for both the quadratic and parabolic failure criteria. α is assumed to be 0.5, 1 and 2.

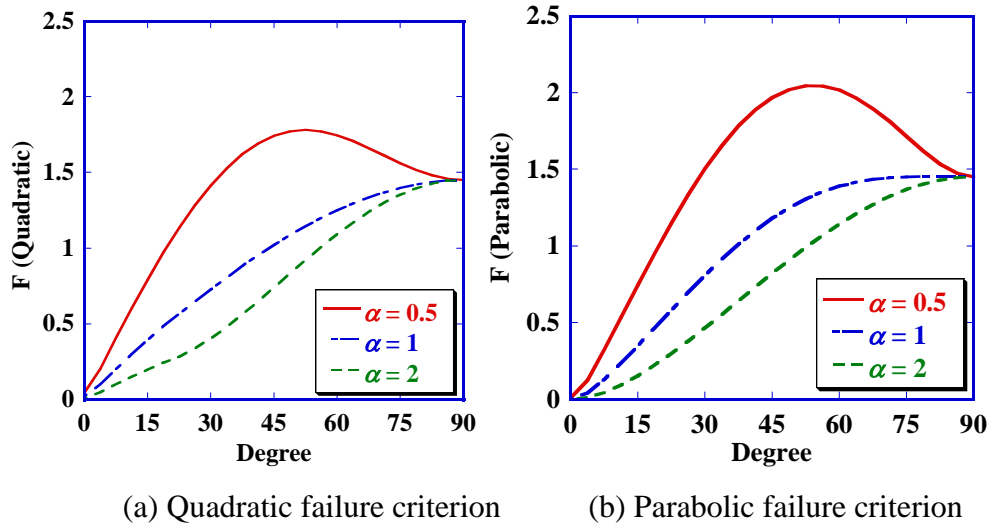


Fig.7 Normalized equivalent interfacial stress (F) as a function of angle θ with assumed values of α for the cruciform-90 specimen under (a) the quadratic failure criterion and (b) the parabolic failure criterion.

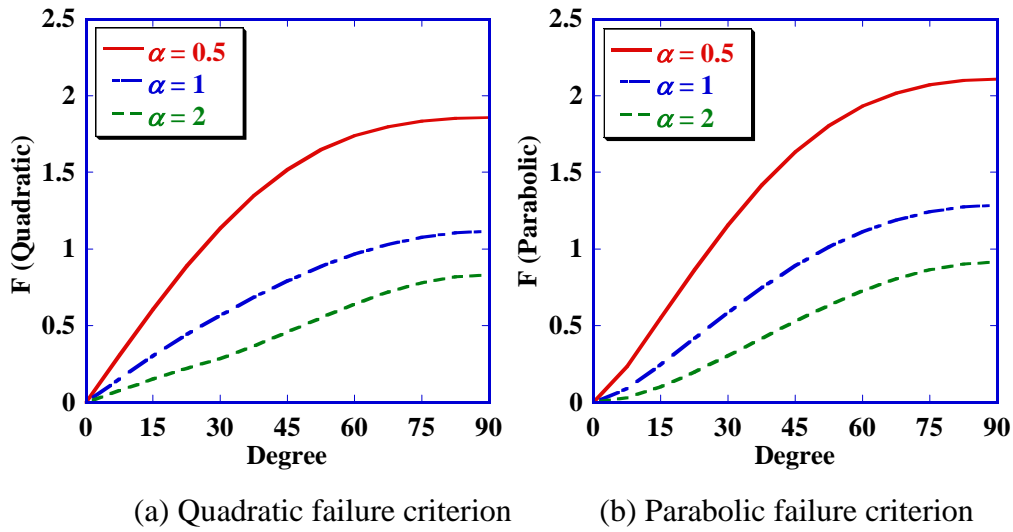


Fig.8 Normalized equivalent interfacial stress (F) as a function of angle θ with assumed values of α for the cruciform-45 specimen under (a) the quadratic failure criterion and (b) the parabolic failure criterion.

In the cruciform-90 specimen, at angle $\theta=90^\circ$, because no interfacial shear stress exists and the stress state is pure tensile, the normalized equivalent interfacial stress F is the same value regardless of α . In both cruciform-90 and cruciform-67.5 specimens, when we assume small α (the interfacial shear strength is smaller than the interfacial tensile strength), the maximum F is taken by θ ranging from 45° to 60° and the point may be the initiation point. On the other hand, in the cruciform-45, cruciform-35 and cruciform-22.5 specimens, it is implied that $\theta=90^\circ$ point is the debonding initiation point.

We can also calculate Y_n by using the experimentally-obtained σ_{spe} and by assuming the value of α . Because Y_n is the material constant, the same value should be derived regardless of the cruciform angle. If we assume a right value for α and if we choose a proper interfacial failure criterion, we have the same Y_n from different cruciform angles. This procedure may be used for determination of Y_n , α and selection of the interfacial failure criterion.

Figures 9 and 10 show the relation between Y_n and α (assumed) by using the experimentally-obtained σ_{spe} in the cases of the quadratic failure criterion and the parabolic failure criterion, respectively.

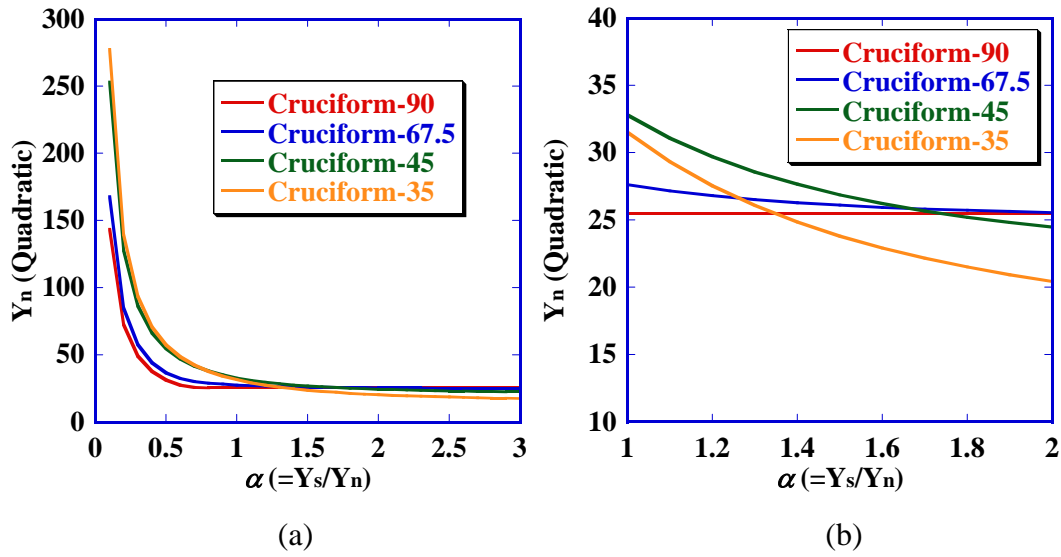


Fig.9 Normalized equivalent interfacial stress (Y_n) as a function of α in the case of the quadratic failure criterion. (a) Overall tendency and (b) magnified view in the range of $1 < \alpha < 2$ where the curves may intersect each other

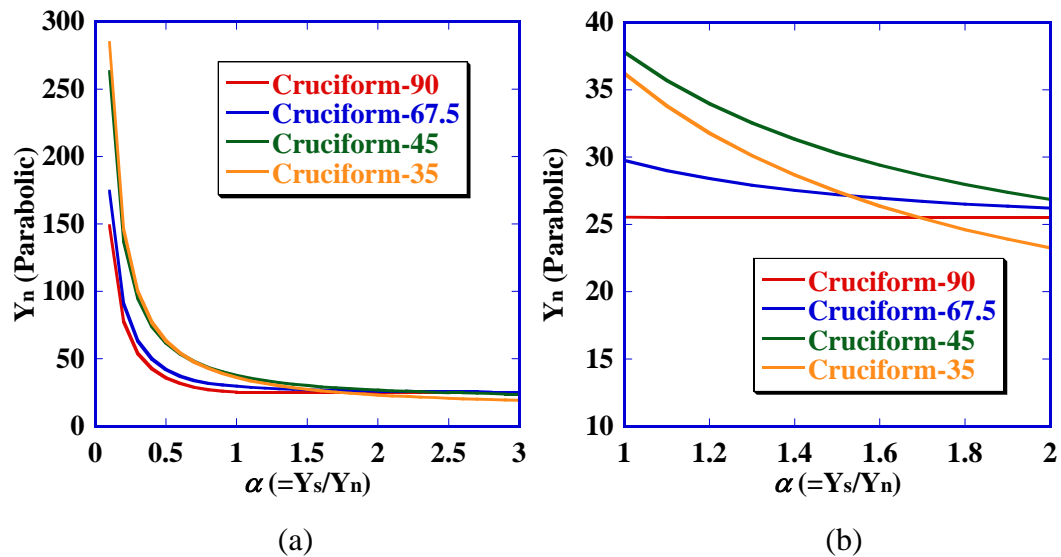


Fig.9 Normalized equivalent interfacial stress (Y_n) as a function of α in the case of the parabolic failure criterion. (a) Overall tendency and (b) magnified view in the range of $1 < \alpha < 2$ where the curves may intersect each other

Although it is considered that if we choose a right interfacial failure criterion, the Y_n - α curves from different cruciform angles intersect each other at the right value of α , practically they do not because of the uncertainty of the experimentally-obtained average specimen stress at interfacial debonding σ_{spe} . However, it seems that $\alpha=1.3$ - 1.8 in the quadratic failure criterion (Fig.9(b)) and $\alpha=1.5$ - 2.1 in the parabolic failure criterion (Fig.10(b)). Anyway, α is higher than 1 and it can be considered that the value of the interfacial shear strength is higher than that of the interfacial tensile strength, and that the debonding initiation point is $\theta=90^\circ$.

If we assume that $\alpha=1.5$, $Y_n=26\text{MPa}$ in the case of the quadratic failure criterion and 28MPa in the case of the parabolic failure criterion. Figure 11 shows the relation between the normal and shear stresses at debonding initiation. In deriving this figure,

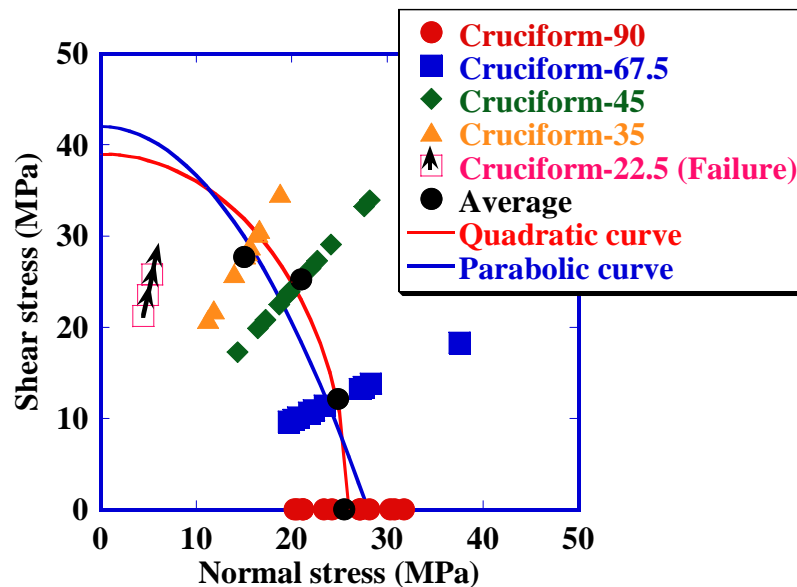


Fig.11 Interfacial failure envelopes (criteria) with experimental results

Conclusion

We conducted cruciform specimen test by varying the cruciform angles to make various interfacial stress state for glass fiber/epoxy composite. We determined the interfacial failure initiation location by introducing two interfacial failure criteria, the quadratic failure criterion and the parabolic failure criterion, using the experimentally-obtained debonding initiation stress and FEM results. It was implied that the value of the interfacial shear strength is higher than that of the tensile strength, and that the interfacial failure initiates from $\theta = 90^\circ$ location for all cruciform specimens tested in this work.

References

1. J.-K.Kim and Y.-W.Mai, Engineered Interfaces in Fiber Reinforced Composites, Elsevier, 1998
2. G.P.Tandon, R.Y.Kim and V.T.Bechel, Evaluation of Interfacial Normal Strength in a SCS-0/Epoxy Composite with Cruciform Specimens, Composites Science and Technology, 60, 2281-2295, 2000
3. S.Ogihara, Y.Sakamoto and J.Koyanagi, Evaluation of Tensile Strength in Glass Fiber/Epoxy Resin Interface using the Cruciform Specimen Method, Transactions of the Japan Society of Mechanical Engineers, 75, 49-55, 2009 (in Japanese)
4. J.Koyanagi, H.Kato and S.Ogihara, Analyses for Establishing Failure Criterion on Fiber/Matrix Interface using Cruciform Specimen Test, Materials System, 27, 63-69, 2009 (in Japanese)